New twists to Einstein's two-slit experiment: complementarity vis-a-vis the causal interpretation

1989 J. Phys. A: Math. Gen. 22 3253

(http://iopscience.iop.org/0305-4470/22/16/016)

J. Phys. A: Math. Gen. 22 (1989) 3253-3266. Printed in the UK

New twists to Einstein's two-slit experiment: complementarity *vis-à-vis* the causal interpretation

D Home† and P N Kaloyerou‡

† Physics Department, Bose Institute, Calcultta 700009, India
‡ Laboratoire de Physique Theorique§, Institute Henri Poincaré, 11 rue Pierre et Marie Curie, 75231 Paris, Cedex 05, France

Received 19 October 1988

Abstract. We consider the new adaptations of Einstein's two-slit experiment in terms of recently performed experiments with neutrons, and analyse them in the light of the complimentarity principle. We constrast this with the description in terms of the de Broglie-Bohm causal interpretation.

1. Introduction

In recent years there has been renewed interest in conceptual ramifications of Einstein's two-slit experiment [1-3], particularly in view of the experimental realisation of some of its new variants. In the present paper we seek to analyse critically the interpretation of these experiments from the point of view of the complementarity principle and contrast this with the description in terms of the de Broglie-Bohm causal interpretation. We also comment on some interesting issues raised by these experiments.

Einstein's two-slit experiment (figure 1) has now become a classic example for exhibiting the peculiar particle-wave duality of the quantum theory. It is well known that using the arrangement of figure 1, Einstein sought to determine the photon (electron, etc) trajectory without destroying the interference pattern. Equally well known is Bohr's rebuttal using the position-momentum uncertainty relations. The

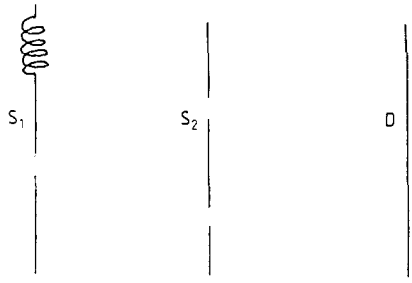

Figure 1. Einstein's low-intensity two-slit experiment. A spring is attached to screen S_1 allowing the determination of the photon trajectory by measurement of the 'momentum kick' to the screen.

§ CNRS/UA no 769.

0305-4470/89/163253+14$02.50

important point here is that this experiment (and other hypothetical experiments proposed by Einstein to attack the completeness of the Copenhagen formalism) dealt with the mutually exclusive situations of either perfect particle knowledge or perfect wave knowledge. Surprisingly 'in-between experiments' were not considered until the interesting 1979 analysis of Wootters and Zurek [4]. Using the hypothetical arrangement of figure 1 they showed that it is possible to obtain partial wave knowledge and partial particle knowledge from the same experimental arrangement. Indeed, they arrived at the surprising result that it is possible to determine with 99% certainty the photon trajectory whilst still retaining a significant interference pattern. They concluded that Bohr's complementarity principle was limited and not able to properly accommodate such 'in-between experiments'. Thus, they were led to state their version of the complementarity principle [4, p 481]: 'The sharpness of the interference pattern can be regarded as a measure of how wave-like the light is, and the amount of information we have obtained about the photons' trajectories can be regarded as a measure of how particle-like it is'. The question immediately arises as to whether or not the above statement is merely an extension of the complementarity principle to 'in-between experiments' or whether it is consistent with Bohr's complementarity at all. To answer this question we must consider Bohr's complementarity principle.

2. The complementarity principle

In this short paper we cannot hope to do justice to the subtleties and generality of Bohr's thesis but refer the reader to Bohr's original writing, particularly [3] but also [5–7]. We will therefore limit ourselves to short extracts from Bohr's writings which we feel best characterise complimentarity in the context of this discussion.

In [3, p 210] Bohr writes 'however far the phenomena transcend the scope of classical physical explanation the account of all evidence must be expressed in classical terms'. He continues, 'this crucial point ... implies the impossibility of any sharp separation between the behaviour of atomic objects and the interaction with the measuring instruments which serve to define the conditions under which the phenomena appear. ... Consequently evidence obtained under different experimental conditions cannot be comprehended within a single picture but must be regarded as complementary in the sense that only the totality of the phenomena exhausts the possible information about the objects. Under these circumstances an essential element of ambiguity is involved in ascribing conventional physical attributes to atomic objects as is at once evident in the dilemma regarding the corpuscular and wave properties of electrons and photons where we have to make do with contrasting pictures each referring to an essential aspect of empirical evidence.

In another article [5, p 90] Bohr writes 'As repeatedly stressed the principal point is here that such measurements demand mutually exclusive experimental arrangements'.

Extrapolating from the above it seems to us that Bohr would have regarded the 'in-between experiments' as simply experiments which do not allow the unambiguous definition of either wave-like or particle-like properties, and that he continually emphasised that such classical concepts (language) could only be used in the context of an experiment in which they could be unambiguously defined. Thus, he also emphasised that the experimental arrangement and quantum system should be viewed as a whole, not analysable into separate parts. Indeed, he maintained that such an analysis was impossible [3, p 235]. In other words, any attempt to associate with a

quantum system alone the attribute of wave or particle is meaningless. Only by consistently maintaining this position, which amounts to denying the possibility of describing the underlying physical reality, could Bohr consistently reconcile the Copenhagen interpretation with Einstein's probing experiments.

We must conclude therefore that the Wootters and Zurek definition of complementarity is not consistent with that of Bohr. Statements such as 'how wave-like' or 'how particle-like' the nature of light surely have no meaning in the context of Bohr's complementarity. What this highlights, as indeed did the whole analysis of Wootters and Zurek and the actual experiments which followed, is the need for a new unambiguous way of talking about quantum experiments. This is in agreement with another conclusion of Wootters and Zurek. The present authors would go further and suggest the need for a description of underlying physical reality in terms of a clear unambiguous well defined model. Such a model exists, namely the de Broglie-Bohm causal interpretation. To exemplify our point we shall give a brief review of actual experiments with neutrons confirming the predictions of Wootters and Zurek and contrast their descriptions with that of the causal interpretation.

In passing we note that the first confirmation of the Wootters and Zurek result was by Mittelstaedt *et al* [8] using a modified Mark-Zender interferometer with a variable partially reflecting mirror to recombine the two photon beams. However, the principle remains the same for the more recent neutron interferometer experiments and, because of their simplicity, we will therefore only consider the latter.

3. Neutron interferometer experiment with static absorber

We consider first the neutron interferometer arrangement of figure 2 with a static absorber in one of the paths and with only one neutron (on average) passing through the instrument at any one time. This experiment has been performed by Rauch and Summhammer [9].

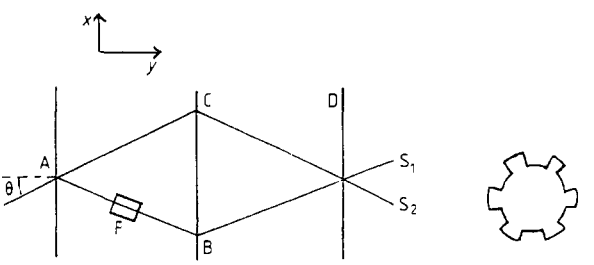

Figure 2. Neutron interferometer. F may be either a static absorber or (right) a time-dependent absorber having 100% absorbing efficiency.

The static absorber (attenuator) reduces the intensity of one of the neutron beams. Depending on the degree of attenuation, a neutron path can be determined with high or low probabilty (50% for the usual no-attenuation case).

Following Greenberger [10] we can imagine a screen D recording an interference pattern, which in practice is determined by counters at S_1 and S_2, to simplify the discussion. The appropriate wavefunction is a superposition of the attenuated-beam and

unattenuated-beam wavefunctions,

$$\psi = \sqrt{a}\psi_B + \psi_C \exp(i\chi) \tag{1}$$

where a, $0 < a < 1$, is the probability for a neutron to pass through the static absorber and χ is the phase difference. The intensity is given as usual by

$$I = |\psi|^2 = a|\psi_B|^2 + |\psi_C|^2 + 2\sqrt{a}\psi_B\psi_C \cos\chi. \tag{2}$$

The possibility of determining the neutron path with high probability whilst retaining a significant but reduced-contrast interference pattern is clearly indicated by the proportionality of the beam intensity to a, whilst the amplitude of the interference term is proportional to a. Rauch and Summhammer were able to achieve attenuation as low as 0.9%. In other words, the neutron path can be determined with 99% certainty and yet retain an observable interference pattern — a striking result indeed.

Counter-intuitive as quantum mechanics often is, are we not left with a mental wrestling match between the two mutually exclusive classical concepts of wave and particle? Or are we happy to follow Bohr and refuse to grasp the underlying mechanism at all or, worse, simply to live with the ambiguous use of wave and particle concepts?

Greenberger and Yasin [10] have replaced the rigorous information theory analysis of Wootters and Zurek by a simpler quantification of the wave and particle knowledge obtainable from a single experiment in terms of a single parameter. Since their results are very close to those of Wootters and Zurek, and since the treatment in terms of a single parameter is more convenient for a causal description of this experiment, we shall make use of it in this section. We thus briefly introduce the Greenberger and Yasin analysis.

Replacing the wavefunction (1) by

$$\psi = (R_1 \exp(iK_x x) + R_2 \exp(i\chi)\exp(-iK_x x))\exp(iK_z Z)\exp(-i\omega t) \tag{3}$$

the intensity is given by

$$|\psi|^2 = R_1^2 + R_2^2 + 2R_1R_2\cos(2K_x x - \chi) \tag{4}$$

where χ is again the phase difference. Greenberger and Yasin defined the contrast of the interference pattern, representing wave behaviour, as

$$W = \frac{2R_1R_2}{R_1^2 + R_2^2}$$

and that representing particle behaviour as

$$P = \frac{|R_1|^2 - |R_2|^2}{|R_1|^2 + |R_2|^2}.$$

The ingenious trick is to represent R_1 and R_2 in terms of a single parameter, say β,

$$R_1 = \alpha\cos\beta \qquad R_2 = \alpha\sin\beta \tag{5}$$

so that $W = \sin(2\beta)$ and $P = \cos(2\beta)$. They were then able to express the dual wave and particle knowledge by

$$P^2 + W^2 = 1.$$

We note that the restriction to wave and particle knowledge is certainly consistent with Bohr's complementarity, but we can go no further within the standard formalism.

Let us proceed therefore with the description in terms of the de Broglie-Bohm causal interpretation, after first recollecting its essential features. We begin by substituting $\psi = R\exp(iS/\hbar)$ into the Schrödinger equation, which allows its decomposition into two real equations; a continuity equation and a Hamilton-Jacobi-type equation. $R = R(x, t)$ and $S = S(x, t)$ are regarded as two real fields which codetermine each other, as reflected by the complex nature of the wavefunction. Comparison of the Hamilton-Jacobi equation with its classical counterpart reveals an extra term, which Bohm called the quantum potential, Q,

$$Q(x_1 t) = -\frac{\hbar^2}{2m}\frac{\nabla^2 R(x_1 t)}{R(x_1 t)}. \tag{6}$$

Electrons, neutrons, etc, are assumed to be real definite particles in the classical sense, and these are guided by the quantum potential. By analogy with classical Hamilton-Jacobi theory the momentum is assumed to be given by ∇S. Particle trajectories can be obtained by integrating $v = \nabla S/m$, with given initial particle positions. In the quantum theory these cannot be measured without disturbing the momentum, thereby changing the whole nature of the experiment, and these are the hidden parameters of the causal interpretation. Instead, we must assume initial particle positions, and as long as these are chosen in accordance with the initial probability density $\psi^*(x, t)\psi(x, t)$ we shall obtain consistent results. The form of the quantum potential is determined as much by the experimental apparatus (environment) as by the particle itself. Thus, the quantum particle and apparatus form a whole in just the way Bohr brilliantly recognised, only the description is achieved with a simple, unambiguous and well defined model which does away with the need for the subtle and complex (and perhaps physically unreasonable) rationale of Bohr's complementarity.

The use of plane waves for the description of interference phenomena is often adequate, but such solutions are nevertheless only idealisations. To proceed with a causal description it is more interesting and more realistic to use wavepackets. In particular, Gaussian wavefunctions serve adequately for this purpose. We shall continue to use the Greenberger simplification of replacing the final crystal face by a screen, as we are only concerned with describing the effects of the attenuation of one of the beams, and since a causal description of neutron interferometry has already been given by Dewdney [11] (see also an earlier article on the causal description of optical interference [12]). Because plane waves have served as such useful idealisations we shall, however, return to a brief description of plane wave interference in terms of the causal interpretation. Thus, consider the superposition of two Gaussian wavefunctions

$$\psi_1 = R_1\left(\frac{2\pi}{\Delta x_0^2 + i\alpha t}\right)^{1/2}\exp\left(-\frac{(x + x_0 - vt)^2}{2\Delta x^2}\right)\exp\left(\frac{i\alpha t(x + x_0 - vt)^2}{2\Delta x_1^2}\right)$$
$$\times\exp[iK(x + x_0) - i\omega t + iK_y] \tag{7}$$

$$\psi_2 = R_2\left(\frac{2\pi}{\Delta x_0^2 + i\alpha t}\right)^{1/2}\exp\left(-\frac{(x - x_0 + vt)^2}{2\Delta x^2}\right)\exp\left(\frac{i\alpha t(x - x_0 + vt)^2}{2\Delta x_1^2}\right)$$
$$\times\exp[iK(x - x_0) - i\omega t + iK_y + i\chi]. \tag{8}$$

ψ_1 is a Gaussian with centre at $-x_0$ at $t = 0$, moving in the $+x$ and $+y$ directions and is of half-width Δx_0. ψ_2 is a packet of the same width Δx_0, with centre at $+x_0$ at time $t = 0$, moving in the $-x$ and $+y$ directions. The amplitudes R_1 and R_2 are still given

by (5) and characterise the attenuation of the beams in terms of β. The total wavefunction is

$$\psi = \psi_1 + \psi_2$$

giving a probability density $\psi^*\psi = R^2$,

$$R^2 = \frac{2\pi}{(\Delta x_0^4 + \alpha^2 t^2)^{1/2}}\left[R_1^2 \exp\left(-\frac{(x + x_0 - vt)^2}{\Delta x^2}\right) + R_2^2 \exp\left(-\frac{(x - x_0 + vt)^2}{\Delta x^2}\right)\right.$$
$$+ 2R_1R_2 \exp\left(-\frac{(x^2 + x_0^2 + v^2t^2 - 2\alpha vt)}{\Delta x^2}\right)$$
$$\left.\times \cos\left(2Kx - \chi + \frac{2\alpha tx(x_0 - vt)}{\Delta x_1^2}\right)\right] \tag{9}$$

with

$$\alpha = \frac{\hbar}{m} \qquad \Delta x^2 = \left(\Delta x_0^2 + \frac{\alpha^2 t^2}{\Delta x_0^2}\right) \qquad \Delta x_1^2 = (\Delta x_0^4 + \alpha^2 t^2).$$

The causal description proceeds by equating $R \exp(iS/\hbar)$ to ψ, from which we can obtain the quantum potential (6),

$$Q(x_1 t) = \frac{x^2}{\Delta x_0^4} = \frac{1}{\Delta x_0^2} - \frac{x}{\Delta x^2}\frac{N(x_1 t)}{J(x_1 t)} - \frac{1}{4}\frac{N(x_1 t)}{J(x_1 t)^2} + \frac{1}{2}\frac{M(x_1 t)}{J(x_1 t)} \tag{10}$$

with

$$N(x_1 t) = -R_1^2 g \exp(-gx) + R_2^2 \exp(gx) - 2\left(2K + \frac{2\alpha t(x_0 - vt)}{\Delta x_1^2}\right) R_1R_2$$
$$\times \sin\left(2Kx - \chi + \frac{2\alpha xt(x_0 - vt)}{\Delta x_1^2}\right)$$

$$M(x_1 t) = R_1^2 g^2 \exp(-gx) + R_2^2 g^2 \exp(gx) - 2\left(2K + \frac{2\alpha t(x_0 - vt)}{\Delta x_1^2}\right)^2 R_1R_2$$
$$\times \cos\left(2Kx - \chi + \frac{2\alpha xt(x_0 - vt)}{\Delta x_1^2}\right)$$

$$J(x_1 t) = R_1^2 \frac{\exp(-2x(x_0 - vt)}{\Delta x^2}\Big) + R_2^2 \exp[2x(x_0 - vt)] + 2R_1R_2$$
$$\times \cos\left(2Kx - \chi + \frac{2x\alpha t(x_0 - vt)}{\Delta x_1^2}\right)$$

where

$$g = \frac{2(x_0 - vt)}{\Delta x^2}.$$

From (5) we see that $\beta = \pi/4$ represents equal beam intensities and corresponds to the usual two-slit case with a maximum-contrast interference pattern. Figure 3 shows 3D plots of the intensity R^2, the quantum potential and plots of the corresponding trajectories.

As we have said, particle trajectories can be obtained by integrating $v = \nabla S/m$, with assumed initial particle positions, which in the present case means integrating the following differential equation, assuming a Gaussian distribution of initial particle

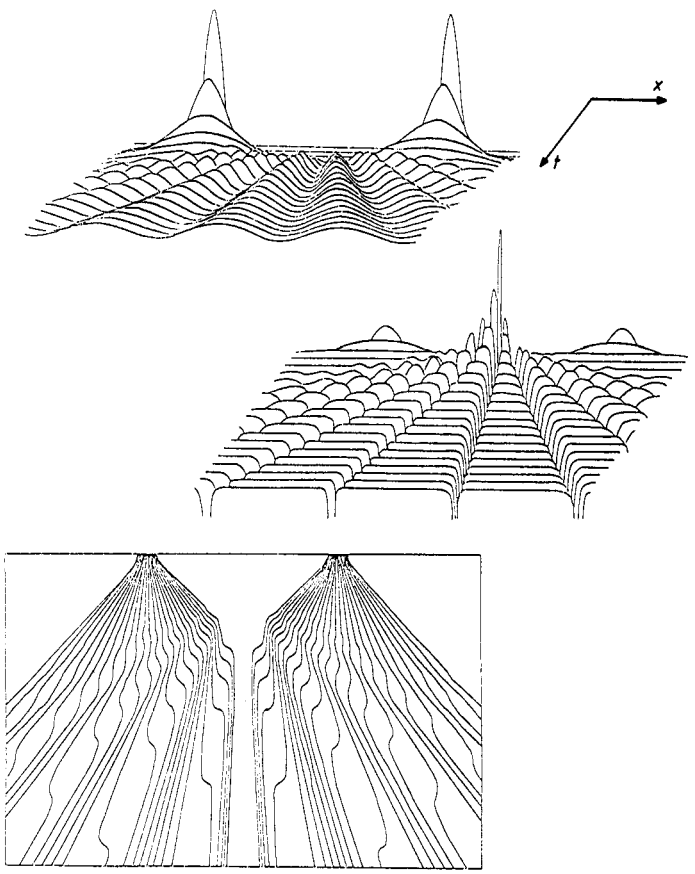

Figure 3. Top: the intensity R^2 for two superposed Gaussian wavefunctions, as viewed from the screen. Middle and bottom: the corresponding quantum potential and trajectories. $\beta = 0.5\pi/2$, which is the usual case of equal-beam intensities giving maximum contrast interference. Phase $\chi = 0$, maximum $t = 1.9 \times 10^{-8}$, with the other constants having values $K = 10^7$ rad m^{-1}, $\Delta x_0 = 6 \times 10^{-9}$ m and $x_0 = 6 \times 10^{-8}$ m.

positions at each slit (i.e. the probability distribution given by (9) for $t=0$):

$$\boldsymbol{r}(t)=x(t)\boldsymbol{i}+y(t)\boldsymbol{j} \qquad \frac{\mathrm{d}y}{\mathrm{d}t}=\frac{\hbar K_y}{m} \qquad \therefore y(t)=\frac{\hbar K_y t}{m}+c$$

$$\begin{aligned}\frac{\mathrm{d}x}{\mathrm{d}t}=&-\frac{2\alpha(x_0-vt)}{\Delta x^2(L^2+H^2)}\left[(R_1^2+R_2^2)\tan(\omega)\left(\frac{2\pi}{\Delta x_1^2}\right)(L\Delta x^2-H\alpha t)\right.\\&\left.-(R_1^2-R_2^2)\left(\frac{2\pi}{\Delta x_1^2}\right)(L\alpha t+H\Delta x^2)\right]\\&+\frac{\alpha}{L^2+H^2}\left[2K+\frac{2\alpha t(x_0-vt)}{\Delta x_1^2}\right]\left[(R_1^2-R_2^2)\sec^2(\omega)\left(\frac{2\pi}{\Delta x_1^2}\right)\right.\\&\left.\times(L\Delta x^2-H\alpha t)-2R_1R_2\tan(\omega)\sec(\omega)\left(\frac{2\pi}{\Delta x_1^2}\right)(L\alpha t+H\Delta x^2)\right]\\&+\frac{\alpha^2 tx}{2\Delta x_1^2}\end{aligned} \tag{11}$$

$$H=2A(R_1^2-R_2^2)\tan(\omega)-2B(R_1^2+R_2^2)-4BR_1R_2\sec(\omega)$$

$$L=2B(R_1^2-R_2^2)\tan(\omega)+2A(R_1^2+R_2^2)+4AR_1R_2\sec(\omega)$$

$$\omega=2Kx-\chi+2\alpha xt\frac{(x_0-vt)}{\Delta x^2}$$

$$A=2\pi\frac{\Delta x_0^2}{\Delta x_1^2} \qquad B=2\pi\frac{\alpha t}{\Delta x_1^2}.$$

This differential equation can be easily integrated numerically using, for example, the standard fourth-order Runge-Kutta method (with adaptive step size).

From figure 3 we see that the intensity of the quantum potential varies in space providing allowed and forbidden paths. Particles entering the troughs (which extend to minus infinity in the case of maximum contrast) experience a force, given by the negative gradient of the quantum potential, which accelerates them through the trough to the next allowed path. We notice that each particle only passes through one trough, and therefore no particle ever crosses the central axis of symmetry ($x=0$ axis). The particles are thus guided to the bright fringes. This replaces the so-called 'particle-wave duality' by a simple well defined model. For the non-relativistic case the quantum object is always a particle, its wave behaviour is determined by the form of the quantum potential, which is very sensitive to the nature of the apparatus (environment).

High or low values of β represent large attenuation of one or other of the beams. Figure 4 shows 3D plots of the intensity R^2, the quantum potential and corresponding trajectories for $\beta=0.3\pi/2$, which represents attenuation of the ψ_2 beam (the right-hand beam in figure 4 and the upper beam in figure 2). In figure 5 we have plotted the intensity R^2 and the quantum potential for three different values of $\beta=0.5\pi/2$, $0.3\pi/2$ and $0.1\pi/2$. We see that the minima of the troughs increase (and are finite) with increasing attenuation, presenting shallower gradients and therefore smaller forces to the particles. This means that more particles can reach regions corresponding to dark fringes in the maximum contrast case. The trajectories plot of figure 4 clearly shows this. Notice that the troughs of the quantum potential have increased minima and shallower gradients on the side of the unattenuated beam, tending more and more to

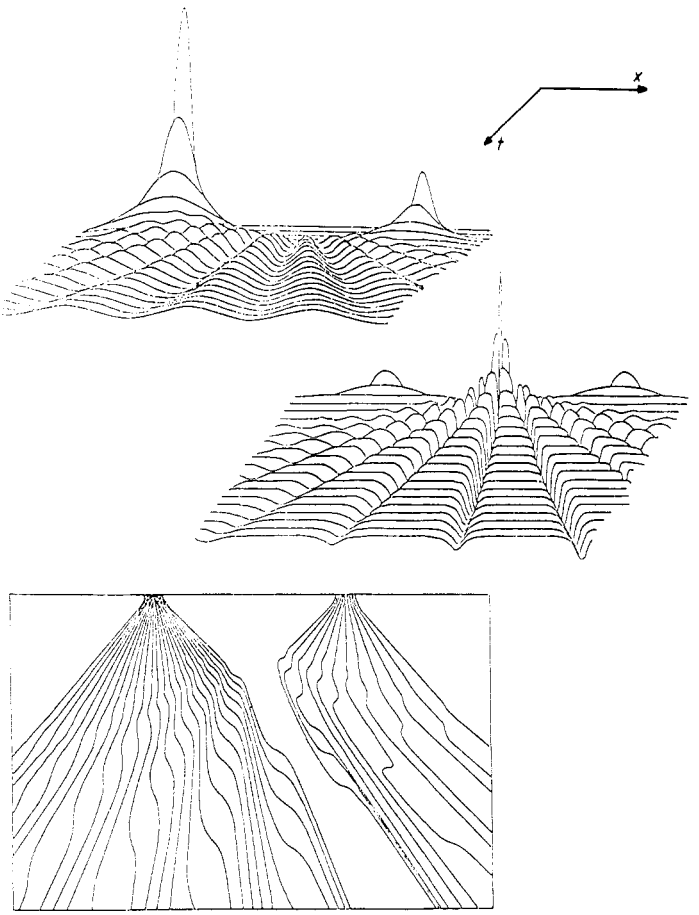

Figure 4. Top. The intensity R^2 for two superposed Gaussian wavefunctions, as viewed from the screen for $\beta = 0.3\pi/2$ (right beam is attenuated). Middle and bottom: the corresponding quantum potential and trajectories, clearly indicating reduced interference as compared with the maximum contrast case. The various constants have the same values as for the plots in figure 3.

a single-slit pattern as the attenuation of the other beam is increased. That a detectable interference pattern is maintained is simply a fact of the experimental configuration which gives rise to a quantum potential where gradients are of a sufficient strength to produce the interference pattern, and there are no strange implications on the basis of our description.

At this point it is worthwhile to pause and consider the magnitudes of the physical quantities involved. Typically, the neutron interferometer is about 8 cm wide and 7 cm in length, and cut from a perfect silicon crystal. The neutron velocities are of the order of $10^3\ \mathrm{m\,s^{-1}}$. The beam cross section may be $1\ \mathrm{cm^2}$ or larger and the two beams separated by a few cm at the middle-crystal face, whilst the width in the longitudinal direction (y direction) is approximately 0.03 cm. These quantities define the dimensions of the wavepacket. For our plots, however, we have chosen numbers to amplify the effects we want to show, and so the numbers shown in figures 5 and 6 should not be taken too literally, except that they reflect the correct order of magnitude of the quantum

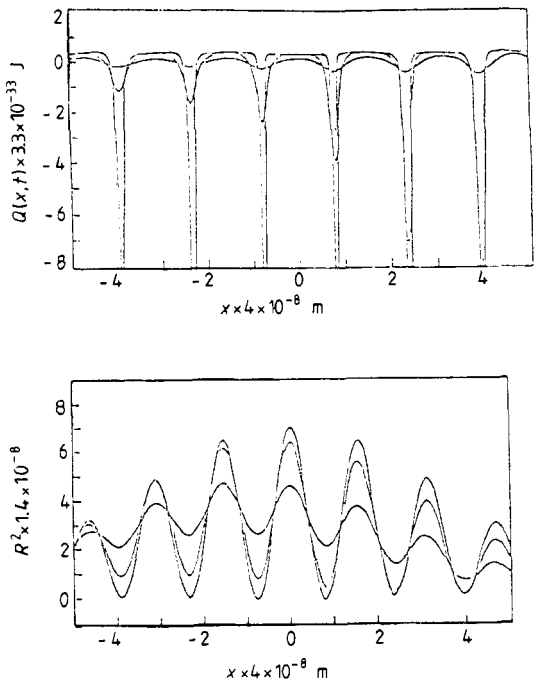

Figure 5. Top. The quantum potential for two superposed Gaussian wavefunctions for three values of $\beta = 0.5\pi/2$, $0.3\pi/2$ and $0.1\pi/2$ (corresponding to a decrease in the intensity of the beam). Bottom: corresponding plot for the probability density R^2 for the same values of β showing reduced contrast with decreasing β. In both cases phase $\chi = 0$, and maximum $t = 1.9\times 10^{-8}$. Other constants have the values $K = 10^7$ rad m^{-1}, $\Delta x_0 = 6\times 10^{-9}$ m and $x_0 = 6\times 10^{-8}$ m.

potential. For our plots we have chosen $K = 10^7$ rad m^{-1} $\Delta x_0 = 6\times 10^{-9}$ m and $x_0 = 6\times 10^{-8}$ m.

Briefly, let us return to consider plane-wave interference. Again, equating $R\exp(iS/\hbar)$ to the wavefunction (3) we can obtain the quantum potential corresponding to the superposition of two plane waves:

$$Q(x,t) = \frac{\hbar^2}{2m}\left(\frac{K^2\sin^2(2Kx-\chi)}{[1/\sin(2\beta)+\cos(2Kx-\chi)]^2} + \frac{2K^2\cos(2Kx-\chi)}{1/\sin(2\beta)+\cos(2Kx-\chi)}\right) \tag{12}$$

which we have plotted in figure 6 for $\beta = 0.499\pi/2$, $0.3\pi/2$ and $0.1\pi/2$. In the case of maximum contrast, $\beta = 0.5\pi/2$, the trough widths become negligible (which is why we have actually plotted for $\beta = 0.499\pi/2$ instead), still extending to $-\infty$, and zero everywhere else. How is this form of the quantum potential to account for the well defined maximum-contrast peaks of R^2 (equation (4)) plotted in figure 6? This is not hard to answer if we notice that we are dealing with a time-independent problem. The intensity R^2 (9), and quantum potential (12), are completely independent of time (and of y). They maintain the same form from the middle-crystal face to the screen. If we further consider the continuity equation, expressing the conservation of probability, then we expect the initial particle distribution at the middle-crystal face to be identical to the final distribution at the screen. In other words, in this case, the quantum potential does not guide the particle at all, but merely reflects the fact that absolutely no particle can reach regions where $R^2 = 0$.

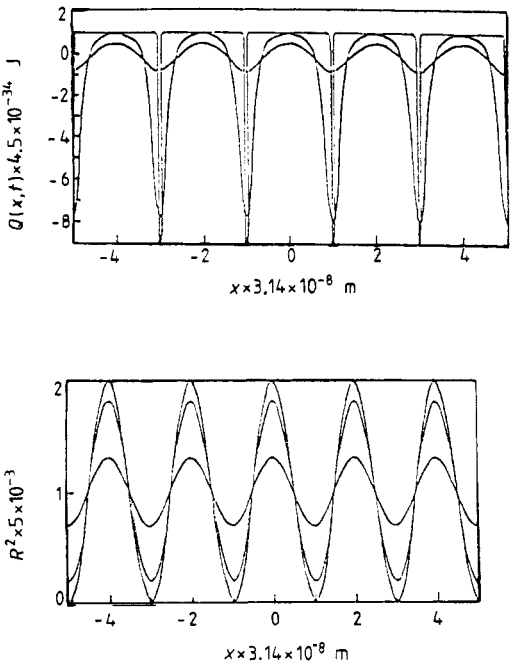

Figure 6. Top: the quantum potential for two superposed plane waves for $\beta = 0.499\pi/2$, $0.3\pi/2$ and $0.1\pi/2$. Bottom: corresponding R^2 plot for two plane waves. Constants have the same values as for the Gaussian case in figure 5.

Again, the reduced contrast when one beam is attenuated is explained by the increased trough minima, and therefore shallower quantum potential gradient, allowing more particles to reach otherwise dark regions (fringes) of the screen.

This point is further substantiated when we work out the trajectories (which we have not plotted here) from the following integrated equations for $x(t)$ and $y(t)$:

$$\boldsymbol{r}(t) = x(t)\boldsymbol{i} + y(t)\boldsymbol{j}$$

$$x(t) = \frac{1}{2}\left(1+\left(\frac{R_1-R_2}{R_1+R_2}\right)^2\right) - \frac{1}{4K}\left[1-\left(\frac{R_1-R_2}{R_1+R_2}\right)^2\right]\chi + \frac{1}{4}\left[1-\left(\frac{R_1-R_2}{R_1+R_2}\right)^2\right]\sin(2Kx(t)-\chi)$$

$$-\frac{\hbar Kt}{m}\left(\frac{R_1-R_2}{R_1+R_2}\right) - G = 0 \tag{13}$$

$$y(t) = \frac{\hbar}{m}K_y t + F$$

where χ is the phase, and G and F are constants of integration.

For the usual maximum-contrast case the trajectories are simply straight lines perpendicular to the crystal face, so that the initial distribution ends up as the final one. When one beam is attenuated, the linear trajectories acquire a slight slope toward the side of the weaker beam, though so small that they remain practically perpendicular to the crystal face and screen over usual experimental distances. As we implied earlier, the more realistic Gaussian is certainly more interesting from the point of view of the causal interpretation.

To summarise, we have accounted for the surprising result of Wootters and Zurek. Simply, in this model, a neutron, electron, etc, is always a particle. The variation in contrast of the interference pattern, due to the variation of the attenuation of one of the beams and, indeed, its very formation, is simply due to the form and intensity of the quantum potential. No paradoxical implications, no ambiguity!

4. Time-dependent absorber

Instead of an attenuator at F we may use a time-dependent absorber (chopper). The result in this case, as has been confirmed by Rauch and Summerhammer [9], is very different from that of the attenuator. Noting that the chopper material absorbs neutrons with 100% efficiency, we can identify definite time intervals when either both paths are available to the neutron, or when only one path is available. During the time interval Δt_2, when both paths are available, the emerging beams are described by the wavefunction ψ_1'

$$\psi_1' = \psi_B + \psi_C \exp(i\chi). \tag{14}$$

In the next interval with only one path available, Δt_1, the emerging beam is described by ψ_2,

$$\psi_2' = \psi_C. \tag{15}$$

The overall wavefunction is a mixture

$$\psi = (\psi_1, \psi_2) \tag{16}$$

where $\psi_1 = \sqrt{a}[\psi_B + \psi_C \exp(i\chi)]$ and $\psi_2 = \sqrt{(1-a)}\psi_c$. The probability a of a neutron to pass the chopper depends on the relative size of Δt_1 (one path available), and Δt_2 (both paths available). The intensity is then given by the usual density matrix prescription

$$I = |\psi_1|^2 + |\psi_2|^2 = a|\psi_B|^2 + |\psi_C|^2 + 2a\psi_B\psi_C \cos\chi. \tag{17}$$

We see that the amplitude of the interference term is reduced in proportion to the attenuation of the beam, and we do not expect to obtain from this experiment as much simultaneous wave and particle knowledge as for the case of the attenuator. This accords with the result of Wootters and Zurek that the maximum simultaneous wave and particle knowledge is obtainable from experimental arrangements described by pure states.

The causal interpretation in this case corresponds to the switching of the quantum potential from the two-path to the one-path form. During the time interval when both paths are available, the quantum potential corresponds to that shown in figure 3 with the characteristic paths in space, as is easily seen by equating $R\exp(iS/\hbar)$ to the wavefunction (9). This gives maximum-contrast interference. During the time interval with only one path available, the quantum potential is obtained by equating $R\exp(iS/\hbar)$ to the wavefunction (15), giving rise eventually to a typical single-path distribution at the screen (i.e. a single hump). This tends to wash out the interference produced during Δt_2. Again the overall pattern is described by (16).

5. Further remarks

The marked difference in the contrast of the interference pattern for the case of a static absorber as compared with the time-dependent absorber is at first sight puzzling. Closer

analysis reveals, however, that the ensemble of neutrons contributing to the interference pattern in the case of the static absorber is bigger than in the case of the time-dependent absorber, even when the experiments are so arranged that the transmission probability a is the same in both cases. To see this, consider first the case of the time-dependent absorber. There will be no contribution to the interference pattern from any neutron entering the interferometer during the time intervals Δt_1, when only one path is available; the neutrons following the free path will contribute only to a characteristic single-path humped distribution, while neutrons taking the alternative path are simply stopped by the chopper, making no registration on the detector at all. Only the ensemble of neutrons made up of those neutrons entering the interferometer during all intervals Δt_2, when both paths are available, contribute to the interference pattern.

In the case of the static absorber having the same probability a for transmission, all neutrons following the free path will contribute to the interference pattern. In addition, those neutrons following the alternative path which pass through the attenuator will also contribute to interference. Those neutrons which are actually absorbed by the attenuator are simply removed from the ensemble contributing to interference, since their absorption corresponds to a localisation measurement. The removal of these absorbed neutrons from the ensemble contributing to interference is taken into account by the probability term a appearing in wavefunction (1) describing this circumstance. Thus, there is a bigger ensemble of neutrons contributing to interference in the case of the static absorber.

To throw some light on the difference between the two ensembles for the different experiments, let us briefly recall the measurement theory of the causal interpretation. In contrast to the usual interpretation there is no wavefunction collapse; rather the particle enters one of the possible eigenstates of a measurement, whilst the others remain empty. That it is overwhelmingly unlikely that the empty packets subsequently interact is due to their inevitable interaction with classical systems possessing many degrees of freedom. In the case of the static absorber the experimental configuration requires that we write a superposition of two wavefunctions. In these low-intensity experiments the physical particle will be represented by only one of the wavefunctions, whilst the other represents an empty wave. The attenuator will have no effect on this empty wave. The quantum potential corresponding to this situation will be that of figure 5, producing reduced-contrast interference.

In the case of the time-dependant absorber represented by a mixture, the wavefunction will be either of two separate forms, so that when the chopper closes one of the paths there will be no accompanying empty wave to produce interference.

Rauch and Summhammer posed a further interesting question concerning whether or not time-dependent absorbtion can possibly reproduce the results of a static absorber. They attempted to answer this question by using the energy-time uncertainty relations. They concluded that when the frequency of the chopper is either very fast or very slow relative to the time of flight of the neutron then the results of the time-dependent absorber approach those of the static absorber.

Is the answer so clear cut, however? The wavefunction, (1), for the static case is a superposition, but wavefunction (11) is a mixture. For the results of the time-dependent absorber to approach those of the static absorber we would expect wavefunction (11), a mixture, to tend to wavefunction (1), a superposition. This implies that wavefunction (11) should be a function of the frequency of the chopper, which it is not. The alternative is that the transition from a mixture to a superposition occurs suddenly at a particular frequency. Either way, the issue is not so clear cut and calls

for further study. In particular, it would be interesting to see the outcome of experiments in which the chopper frequency is made fast or slow (and random).

6. Concluding remarks

We have tried to compare the analysis of new issues raised by recent adaptations of Einstein's two-slit experiment with Bohr's original form of the complementarity principle. Whereas such experiments are certainly consistent with this principle, they further highlight the need for care in the use of classical concepts and language, at least if conceptual consistency is desired. Ultimately, as with the original two-slit (and other) experiments, consistency is achieved only by renouncing the possibility of describing the underlying physical reality. We have contrasted this with the alternative description in terms of the de Broglie-Bohm causal interpretation which provides exactly the simple clear and unambiguous description of underlying physical reality that Bohr considered impossible, even in principle.

In § 5 we focused attention on a further interesting issue raised by these experiments concerning the relation between mixtures and superpositions.

Acknowledgments

DH thanks the Institute Henri Poincaré, Paris, for hospitality during his visit and PNK thanks the Royal Society for financial support. We are grateful to Professor J P Vigier for interesting and stimulating discussions. We also thank Bob Callaghan for help with the computing and Gill Kaloyerou for proofreading and typing the manuscript. DH is partially supported by the Department of Science and Technology, Government of India, under project number SP/52/K-42/88.

References

[1] Jammer M 1974 *The Philosophy of Quantum Mechanics* (New York: Wiley) pp 121-32
[2] Belinfante F J 1975 Measurement and time reversal *Objective Quantum Theory* (Oxford: Pergamon) pp 32
[3] Bohr N 1949 Discussion with Einstein on epistemological problems in quantum mechanics, *Albert Einstein, Philosopher-Scientist* (Evanston, IL: Library of Living Philosophers) pp 201-41
[4] Wooters W K and Zurek W H 1979 *Phys. Rev.* **D 19** 473
[5] Bohr N 1961 *Atomic Physics and Humane Knowledge* (New York: Science Editions)
[6] Bohr N 1934 *Atomic Theory and the Description of Nature* (Cambridge: Cambridge University Press)
[7] Bohr N 1928 *Nature* **121** 78, 580
[8] Mittelstaedt P, Prieur A and Schieder R 1987 *Found. Phys.* **17** 891
[9] Rauch H and Summhammer J 1984 *Phys. Lett.* **104A** 44
[10] Greenberger D M and Yasin A 1988 *Phys. Lett.* **128A** 391
[11] Dewdney C 1985 *Phys. Lett.* **109A** 377
[12] Dewdney C, Phillipides C and Hiley B J 1979 *Nuovo Cimento* B **52** 15